ELSEVIER

Low-resolution structure refinement in electron microscopy

James Z. Chen,[a] Johannes Fürst,[a,b] Michael S. Chapman,[c] and Nikolaus Grigorieff[a,*]

[a] *Department of Biochemistry, Rosenstiel Basic Medical Sciences Research Center, Howard Hughes Medical Institute,
Brandeis University, 415 South Street, Waltham, MA 02454, USA*
[b] *Department of Physiology, University of Innsbruck, Fritz-Pregl Str. 3, A-6020 Innsbruck, Austria*
[c] *Kasha Laboratory, Department of Chemistry and Biochemistry, Institute of Molecular Biophysics, Florida State University,
Tallahassee, FL 32306, USA*

Abstract

A real-space structure refinement method, originally developed for macromolecular X-ray crystallography, has been applied to protein structure analysis by electron microscopy (EM). This method simultaneously optimizes the fit of an atomic model to a density map and the stereo-chemical properties of the model by minimizing an energy function. The performance of this method is characterized at different resolution and signal-to-noise ratio conditions typical for EM electron density maps. A multi-resolution scheme is devised to improve the convergence of the refinement on the global energy minimum. Applications of the method to various model systems are demonstrated here. The first case is the arrangement of FlgE molecules in the helical filament of flagellar hook, in which refinement with segmented rigid bodies improves the density correlation and reduces severe van der Waals contacts among the symmetry-related subunits. The second case is a conformational analysis of the NSF AAA ATPase in which a multi-conformer model is used in the refinement to investigate the arrangement of the two ATPase domains in the molecule. The third case is a docking simulation in which the crystal structure of actin and the NOE data from NMR experiments on the dematin headpiece are combined with a low-resolution EM density map to generate an atomic model of the F-actin–dematin headpiece structure.
© 2003 Elsevier Inc. All rights reserved.

1. Introduction

With the rapid advances in electron microscopy (EM), it is becoming increasingly feasible to study the structure and function of macromolecules at nanometer or even sub-nanometer resolution. The resolution that can be obtained often depends on the sample geometry. For two-dimensional crystals and helical particles, a resolution between 7 and 3.5 Å is typically achieved (for example, Henderson et al., 1990; Miyazawa et al., 1999). The study of highly symmetrical viruses usually yields a resolution between 6 and 10 Å (for example, Bottcher et al., 1997; Chiu and Rixon, 2002). Particles with lower symmetry or no symmetry at all are usually at the low end of the spectrum, with resolution values between 8

and 20 Å (for example, Frank and Agrawal, 2000; Golas et al., 2003). Unless the resolution of the map exceeds 4 Å, it is normally not possible to build an atomic model solely based on the density map. When atomic models for parts of the structure are available, however, the entire structure can be modeled by manually arranging the known parts in the lower-resolution EM map until a visually acceptable solution is achieved. This approach works well at a coarse scale, largely owing to the human mind's remarkable pattern recognition ability. Nevertheless, inconsistencies and errors arise due to inevitable subjective bias. Noise, which is frequently mingled with signal, also hampers the modeling effort.

There have been a number of efforts in developing computational algorithms to facilitate the interpretation of density maps at a molecular scale using atomic models obtained by other means. The helixhunter and foldhunter computer programs (Jiang et al., 2001) use a pattern recognition technique to reveal helical structures

---

* Corresponding author. Fax: 1-781-736-2419.
E-mail address: niko@brandeis.edu (N. Grigorieff).

embedded in a map and to correlate them to known folding templates in order to determine the architecture of the molecule of interest. The Situs package (Wriggers et al., 1999) employs topology-representing neural networks to vector-quantize features in a three-dimensional (3D) model and correlate them with low-resolution map data. The COAN program (Volkmann and Hanein, 1999) optimizes the global density correlation between a 3D model and an observed volume, and it can be optionally supplemented by restraints derived from biochemical and biophysical data. EMFit (Rossmann et al., 2001) and DOCKEM (Roseman, 2000) both employ real-space density-matching procedures to dock rigid atomic models into EM maps.

The refinement of atomic models against high-resolution X-ray and NMR data usually includes stereochemical restraints that are implemented as a molecular mechanical force field (for example, see Brünger et al., 1987). The objective of this work is to explore the use of empirical energy functions derived from the force field to refine atomic models in the context of low-resolution EM structures. For this refinement, entire domains of the atomic structures will be defined as rigid bodies to reduce the degrees of freedom of the model. This approach should provide a more objective and reproducible method that can simultaneously maximize the model–density correlation and optimize inter-/intramolecular interactions. Our approach will be based on the real-space method RSRef (Chapman, 1995), which was originally developed for atomic structure refinement in X-ray crystallography and has recently been applied to EM structural studies (Chen et al., 2001; Gao et al., 2003). The following sections will introduce RSRef and characterize it in the low-resolution domain. Then, its application to several model systems will be presented.

2. Methodology and characterization

The RSRef structure refinement method calculates a density map according to a proposed 3D model. By restricting the effective range of atomic scattering factors, a calculated map can be constructed at a specified resolution. The atomic model is then refined to minimize differences between the calculated and experimental maps. Since the electron microscopy data arise from electron scattering, the experimental EM density map will be different from the model map derived from X-ray atomic scattering factors. It has been shown, however, that this difference does not affect the refinement (Grigorieff et al., 1996), and the original RSRef map calculation based on X-ray atomic scattering factors should still be valid at the resolution of interest in EM.

The RSRef algorithm has been integrated into the X-PLOR package to provide molecular dynamics functionality in the refinement (Chen et al., 1999a; Korostelev et al., 2002). The integrated X-PLOR/RSRef algorithm will herein be referred to as the "real-space molecular dynamics refinement" method, or the RSMD method. Adaptation of this method to the structure refinement using EM maps is straightforward. The refinement protocol normally consists of an initial stage of energy minimization to reduce hard van der Waals contacts among the composing subunits. Known component structures are then fitted into the EM density by treating domains as rigid units, linked to each other by flexible polypeptides. Refinement uses a slow-cooling torsion-angle molecular dynamics protocol with a starting temperature at 1000 K, followed by final energy minimization to fine-tune the structural conformation. The refinement cut-off parameter of RSRef, which limits the number of grid points surrounding each atom for scaling and derivative computation, is set to 8.0 Å, and the calculation cut-off parameter, beyond which the contribution of an atom to the density grid is neglected, is set to 16 Å. Equal weights are applied to balance the stereo-chemical energy and the density-matching term. In parallel to the work described here, similar methodology has been re-implemented as a module for the CNS package (Brünger et al., 1998), and the newer version will be made available once development and validation are complete (Fabiola, Korostelev and Chapman, unpublished).

The performance of the RSMD method is tested with simulated density maps generated using an atomic model of the D2 domain of *N*-ethyl maleimide sensitive factor (NSF) (PDB entry code 1NSF, Yu et al., 1998) (247 residues). To create a variety of conditions that may be encountered with EM density maps, the NSF-D2 map is filtered at different resolution values, ranging from 6 to 40 Å, and Gaussian noise is added to produce signal-to-noise ratios (SNR) varying between 25:1 and 1:25 (ratio of variance). The maps are generated using the SPIDER computer program (Frank et al., 1996) with isotropic grid spacing at 3 Å.

In a first series of tests, density maps containing only one NSF-D2 domain are synthesized. The atomic model is then randomly displaced from its initial location by about 5 Å and subsequently refined against each map by a rigid-body simulated annealing protocol. The result of the refinement is assessed by the model–density correlation coefficient and the root-mean-square deviation (r.m.s.d.) of the model coordinates from their original coordinates before displacement. Given the nanometer resolution and 3 Å map grid, models refined within an r.m.s.d. of 1.5 Å will be deemed acceptable. The results (Fig. 1) show that the model can be brought back close to its original location even with a map at 20 Å resolution and an SNR of 1:4. This simulation indicates that the real-space method can optimize the model–density fit at nanometer resolution and a wide range of SNR
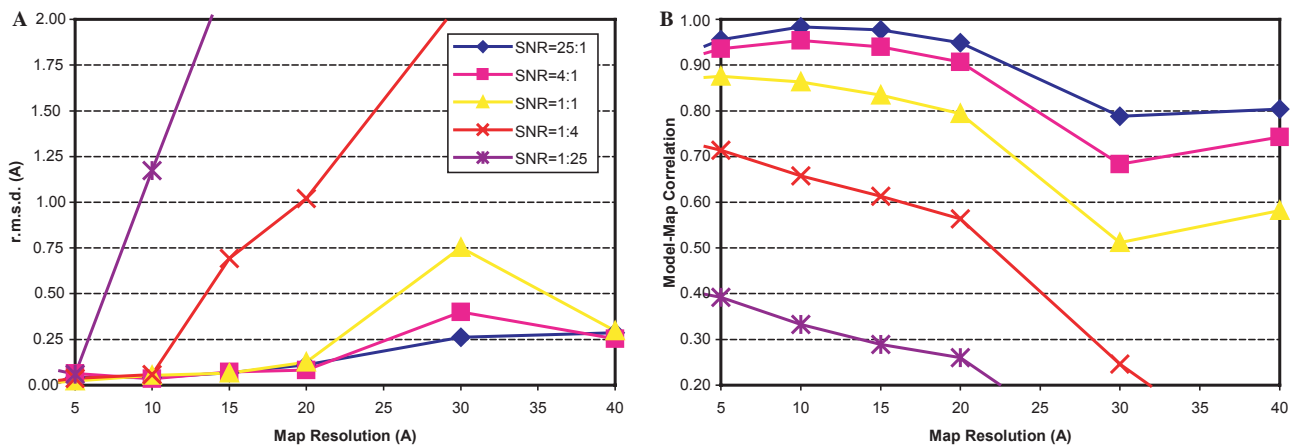
Fig. 1. Characterization of RSMD refinement at various map resolution and SNR values.
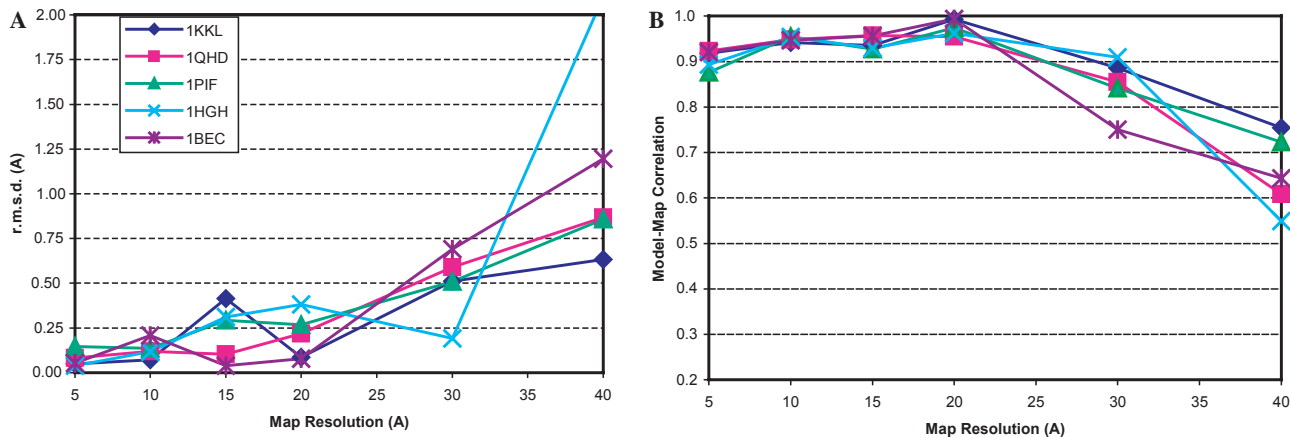

Fig. 2. A series of structures (from the CAPRI project) are used to test the response of the RSMD method to different folding patterns. The SNR in the synthetic maps is set to 1:1. Both the r.m.s.d. and the Model–density correlation statistics indicate that the performance of the method is comparable for various folds across a range of map resolutions.
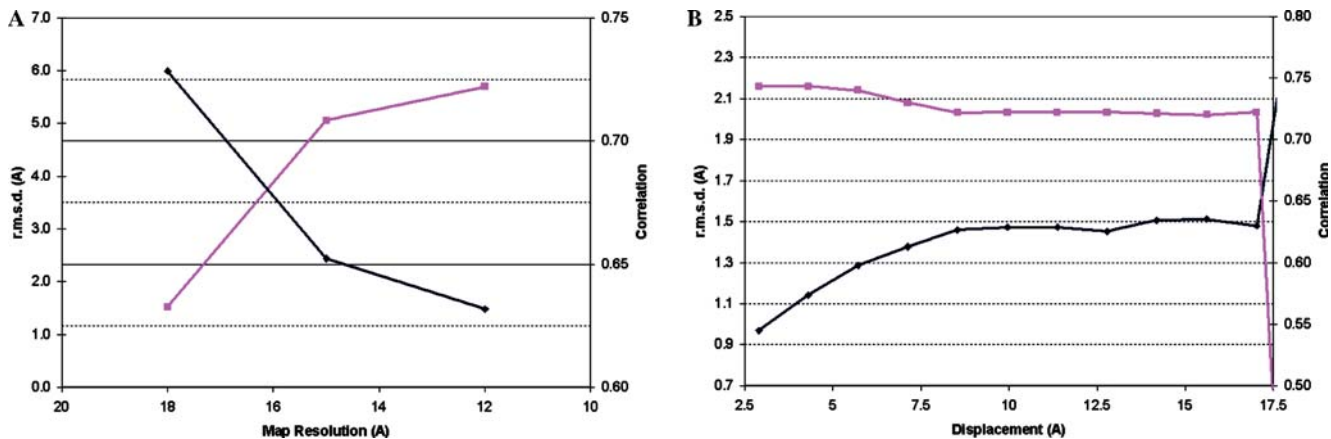

Fig. 3. (A) Progress of a multi-resolution refinement. The initial model is displaced by more than 15.0 Å. B) Test of the convergence radius. The correlation drops dramatically beyond 17.0 Å. In both cases, the root-mean-square deviation (dark blue) is read from the ordinate on the left and the correlation coefficient (purple) is read from the ordinate on the right.
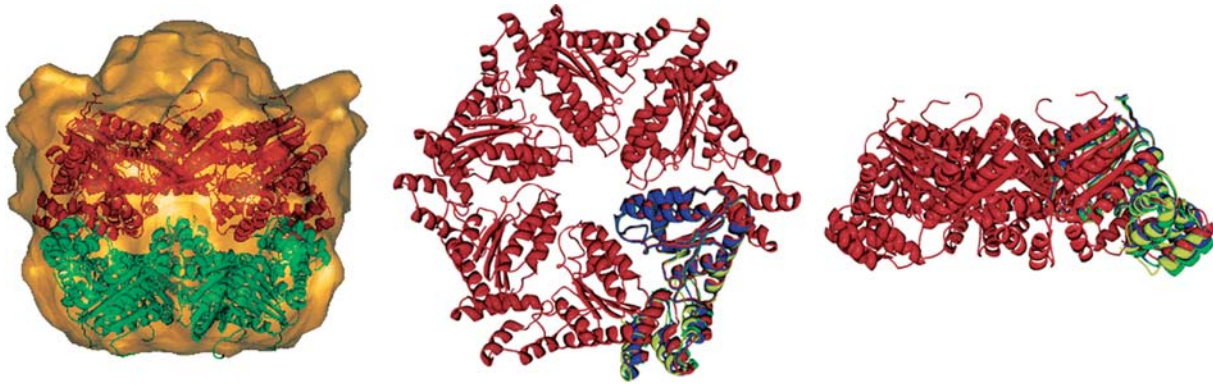
Fig. 4. (A) The D1(green) and D2 (red) hexamers of NSF in the anti-parallel conformation. (B) Multi-conformers of D1 are shown in one subunit (two orthogonal views).

values that include those normally encountered in electron cryo-microscopy [usually above 1:1, according to the common resolution measure of a Fourier Shell Correlation (Harauz and van Heel, 1986; Saxton and Baumeisterm, 1982) of 0.5 at the limiting resolution, calculated between structures derived from two halves of the data set].

Since the accuracy of an RSMD refinement is affected not only by the resolution or noise level of the electron density data, but also by the geometric characteristics of the model structure, further tests have been conducted on a gallery of macromolecules with different folds. The test structures came from those used in the CAPRI contest (Janin et al., 2003), in which the participating research groups applied their computational docking algorithms to predict the conformations of a set of specially selected protein–protein complexes. Only receptor molecules are used in our test, and their PDB codes are 1KKL, 1QHD, 1PIF, 1HGH, and 1BEC. In each case,

synthetic maps are generated from the structure across a range of resolutions with a fixed SNR of 1:1. The model is then randomly displaced (by both translation and rotation as a rigid body) from its original position. The amount of displacement varies between 5.3 and 7.7 Å. Both the r.m.s.d. and the model–density correlation statistics on the refined structures indicate that the performance of the RSMD method is comparable for various folds across a range of map resolutions (Fig. 2).

In the modeling of a multi-subunit complex, it is common that only some of the components are known at atomic detail. This could leave substantial regions in the density map unoccupied. Because the RSMD method optimizes the fit of a model with its surrounding density, it provides a means for local refinement that can still proceed even if the model is incomplete.

In a third series of tests designed to characterize the refinement of a subunit in a larger complex, density maps are generated using the NSF-D2 hexamer that
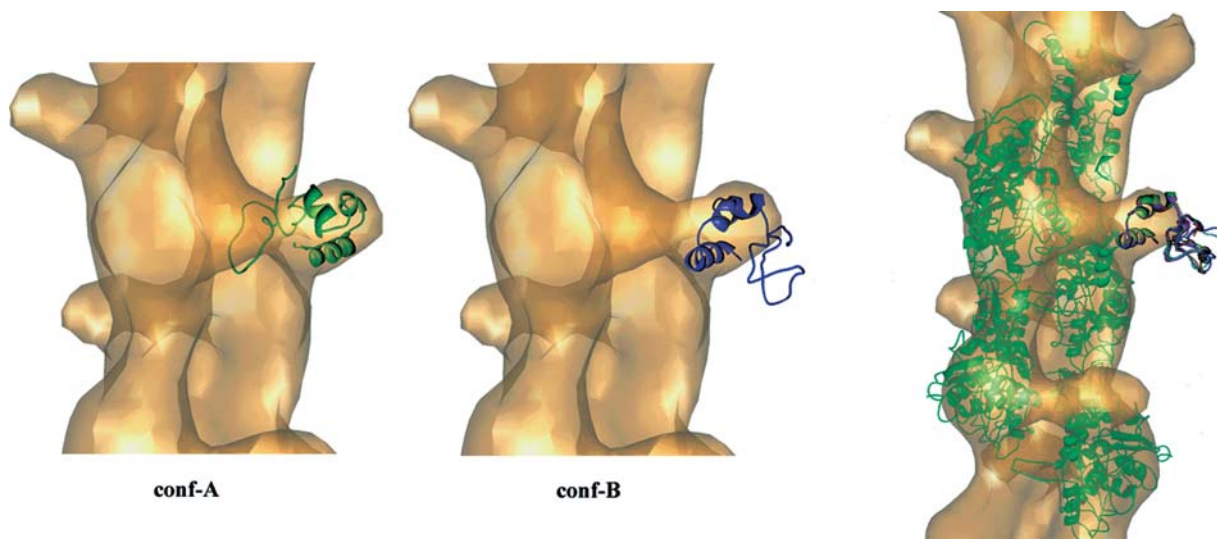

Fig. 5. Two possible conformations of the actin–DHP complex: conf-A and conf-B. The correlation of conf-A with the map is 0.49, while the correlation of conf-B with the map is 0.67 (for the helical domain). The result from multiple rounds of independent refinement with NOE restraints is shown on the right. A threshold has been applied to eliminate noise density in the display.

corresponds to its likely conformation in the biologically active complex (Lenzen et al., 1998; Yu et al., 1998). A monomer is then displaced from its original position within the hexamer and is brought back by RSMD refinement, as before. The remaining five NSF-D2 monomers are omitted during the refinement, thus creating the situation of an incomplete model for the complex. Unlike the previous test, the map resolution is fixed at 12 Å and only the SNR is varied. To evaluate the convergence radius, displacements of up to 20 Å are explored to determine the limit at which refinement progressed towards a false local energy optimum rather than the global optimum. The monomer structure is divided into two rigid-body segments (the catalytic domain of residues 489–665 and the helical domain of residues 673–735). The model is then scrambled via molecular dynamics simulation at a temperature of 800 K and refined against each map. Results partially depend on the starting locations, but the convergence radius appears to be about 10 Å (r.m.s.d.).

To avoid trapping the refinement procedure in local energy minima and to increase the convergence radius of the RSMD method, a multi-resolution refinement scheme is developed. It is motivated by the coarse-to-fine approach frequently used by image analysis algorithms (Rosenfeld, 1984). A lower-resolution map is first calculated by filtering the map at low resolution, and the model is refined against the filtered map. Upon completion, a new map at higher resolution is generated and the refined structure from the previous stage serves as the starting model for the next iteration, until the original map resolution is reached. In the test, the refinement proceeds in three steps at a resolution of 18, 15, and eventually 12 Å (Fig. 3). This multi-resolution scheme indeed reduces the chance of the model being trapped at a local minimum during the refinement. Using the same evaluation criterion (see above), the convergence radius of the method is assessed at around 17 Å at an SNR of 1:4 in the model system. Applications of the RSMD method will be presented below.

3. Helical structure of the flagellar hook

The flagellar hook is a helical assembly of subunits found in the bacterial flagellum where it acts as a universal joint connecting the proton-powered rotary motor and the flagellar filament. The hook monomer (protein FlgE) has three domains bridged by two peptide strands (Morgan et al., 1993). The molecular structure of a central core fragment of FlgE, obtained by removal of terminal regions that are unfolded in the monomeric form, has been solved by X-ray crystallography to 1.8 Å resolution (Samatey et al., 2003), and the density map of the intact hook has been independently determined by electron cryo-microscopy at 9.0 Å reso-

lution (Shaikh et al., 2003a). In its helical hook structure, each monomer has six nearest neighbors that are related by non-crystallographic symmetry (NCS). The goal of the refinement is to fit the atomic structure of the subunit fragments into the EM density map and to examine potential conformational changes.

The crystal structure of the FlgE fragment molecule is manually placed into the map as a rigid body using the modeling program Chimera (Huang et al., 1996) (Model A in Table 1). To optimize the map correlation, a manual adjustment (a hinged rotation operation) is performed, guided by visual inspection (Model B, Shaikh et al., 2003a). Interactions either within the molecule or among the NCS-related neighbors are not considered in this process. The manual modeling indeed improves the overall fit of the density as indicated in the reduction of the energy term E(RRES) (Table 1). The molecular mechanical energy calculation, however, indicates that there exist hard contacts between the two domains of the monomer and among the NCS-related neighbors.

To apply the RSMD refinement, the two major domains of the FlgE fragment molecule are defined as individual rigid bodies connected by flexible peptide chains. Simulated annealing is employed during the structure refinement, allowing the torsion angles in the flexible peptide linkers to vary. In addition, NCS operators are introduced to enforce the symmetry within the helical structure. It is observed (Model C in Table 1) that the model–density match is further improved and the hard van der Waals contacts, both within and between the molecules, are significantly reduced.

4. Conformation of the NSF-D1 domain

NSF is a member of the AAA ATPases family and is involved in several cellular processes, including vesicle fusion and membrane protein trafficking. The D1 and D2 domains of NSF form hexameric rings that are arranged in a double-layered barrel, while the N domain can undergo large conformational changes (Hanson et al., 1997). The crystal structure of the D2 domain has been solved at 1.9 Å resolution (Lenzen et al., 1998; Yu et al., 1998) and consists of the catalytic and helical subdomains. Studies on other AAA ATPases and homology modeling indicate that the folding of the D1 domain is similar to that of the D2 domain. Nevertheless, their relative orientation, either in a parallel or anti-parallel fashion, is still unclear due to the difficulty in crystallizing the entire molecular complex. RSMD refinement is applied in an attempt to determine their possible arrangements using an 11 Å resolution density map derived from single-particle electron cryo-microscopy (Fürst et al., 2003).

Assuming homology between the two domains, we use a copy of the D2 domain to model the structure of

Table 1
Molecular mechanical energy evaluation for various structures

Model	E(BOND)	E(ANGLE)	E(DIHE)	E(VDW)	E(PVDW)	E(RRES)
A	0.990	10.353	3.161	−208.241	0.33E + 8	166.963
B	0.975	10.397	3.169	0.47E + 7	0.29E + 5	161.755
C	0.923	10.351	3.138	−191.355	−14.383	155.835

Model A is the original crystal structure rigidly placed into the map; Model B is the result of separate manual adjustments of the two molecular domains; and Model C is the RSMD refined structure. E(DIHE) is the dihedral energy term; E(PVDW) is the van der Waals contact between the NCS-related subunits; and E(RRES) is the real-space residual target function used in the refinement.

the D1 domain. The model corresponding to the D1 part is manually placed into the map using the modeling program Chimera (Huang et al., 1996). To accommodate for the potentially large conformational differences between the D1 and D2 domains, the multi-resolution approach is applied with successive refinement at 20, 17, 14, and 11 Å resolution cut-offs. In the refinement, the two sub-domains of NSF-D2 are treated as separate rigid bodies (Fig. 4), connected by a flexible linker formed by peptide segment 665:673 (PDB file 1NSF, Yu et al., 1998). Torsion-angle molecular dynamics simulation is applied in the refinement. Because of the unsolved density in the experimental map around the N-terminus and parts of the D1 domain of the NSF molecule, the difference in the model–density correlation between the refined PARA and ANTI conformations is marginal (0.42 versus 0.45) and inconclusive.

Given the multiple conformations observed for the neighboring N domain (Fürst et al., 2003), the D1 domain could also exist in multiple conformations that consist of more subtle differences that are not resolved in the 11 Å density map. To model the D1 domain as an average structure containing multiple conformations, a four-conformer structure is adopted and a multi-conformer refinement (Chen and Chapman, 2001) is applied. In the refinement, each conformer assumes equal occupancy in the structure. The correlation coefficient of the refined multi-conformer structure with the EM density map is 0.44 in the PARA case, and 0.52 in the ANTI arrangement. It indicates that the anti-parallel conformation is more likely for the arrangement of the D1 and D2 hexamers in NSF (Fig. 4), in agreement with Fürst et al. (2003). The above correlation value may seem low at first glance given the good model–density agreement perceived by visual inspection. However, when the same procedure is applied to calculate the model–density correlation for the known D2 domain, the correlation coefficient is only 0.58. Therefore, EM data of higher quality and higher resolution will be needed for a more detailed analysis of the molecular conformation.

5. EM-guided actin–dematin headpiece docking

The actin–dematin headpiece complex provides a test-bed for EM-guided protein–peptide docking. The crystal structure of actin at 2.8 Å resolution (Kabsch et al., 1990) (PDB file 1ATN) is first manually placed into a 20-Å resolution EM density map (Egelman and DeRosier, 2003) and subsequently refined as a rigid body. NCS operators calculated from the map data are included in the refinement to maintain the known helical structure in the filament. Dematin headpiece (DHP) (Frank et al., 2003), the peptide ligand, which is composed of three helices and a flexible tail, is then introduced into the system. Visual inspection identifies an unoccupied density volume where the helical domain of DHP should reside. There are, however, two possible orientations for DHP (Fig. 5). For each case, DHP is manually placed into the density followed by a rigid-body refinement in real space with the actin molecule fixed. The correlation coefficient around the region occupied by the helical domain of DHP is 0.49 for the first conformation (conf-A) and 0.67 for the second (conf-B). The correlation measurement unequivocally indicates that the second arrangement is correct. The structure of the complex is then further refined by assigning each α-helix of DHP as an individual rigid body with the already-refined actin molecule fixed.

There is only weak density corresponding to the tail of DHP, and therefore, the tail tends to extend freely during molecular dynamics refinement. Since the tail should be folded, NOE constraints from NMR experiments are incorporated into the refinement. The model–density correlation was only evaluated for the helical domain. An ensemble of complex structures from multiple rounds of refinement with different initial randomization is shown in Fig. 5. The model–density correlation is above 0.71 for the refined structure. A structure analysis based on chemical properties (Frank et al., 2003) indicates that the residues E68, K71, and K72 of DHP participate in the complex docking by forming an alternating charged "crown" at the binding face. The structure of the refined actin–DHP complex agrees with this conclusion.

6. Discussion

Electron microscopy has become a major technique in the structural study of macromolecules and their complexes. Although atomic resolution is not routinely

achieved, the interpretation of EM density maps at the molecular scale using atomic models available for parts of the maps is feasible. Here, the RSMD refinement method originally developed for X-ray crystallography has been used to refine atomic models against EM density maps. Coupled with the built-in molecular mechanical force fields of X-PLOR (Brünger, 1992a), this method optimizes both model–density fit and stereochemical properties of the atomic model. Unlike visual inspection and manual modeling, this computational method is able to perform structure refinement more objectively and reproducibly. As a demonstration of its application, the RSMD method has been applied to the docking of the structure of flagellar hook protein FlgE into its helical EM map (9 Å resolution), the conformational analysis of NSF (11 Å resolution), and the EM-guided receptor–ligand docking in the actin–DHP complex (20 Å resolution).

Unlike existing model–density docking algorithms, such as SITUS (Wriggers et al., 1999), COAN (Volkmann and Hanein, 1999), EMFit (Rossmann et al., 2001) and DOCKEM (Roseman, 2000), RSMD permits both inter- and intra-molecule conformational changes in the refined structure while observing stereo-chemical restraints. With the flexible selection functions implemented in the X-PLOR package, rigid segments can be easily defined for a small group of atoms or a large chunk of molecular domains. Thus, the RSMD method can be used to investigate structural variability in a molecule.

The RSMD method can also be applied to guide protein–protein docking predictions. To improve the accuracy of such predictions (see CAPRI project; Janin et al., 2003), extra experimental restraints, as, for example, in the form of a single-particle EM density envelope, can be incorporated to reduce the tremendous parameter space of optimization. The docking site and the extent of flexibility of the bound complex can first be identified by an RSMD refinement with the map data, followed by a specially tailored computational algorithm to produce an improved atomic-model prediction. Research on this topic will be reported in a future publication.

The density maps used in the applications were derived from electron microscopy data. In each case, the size of the density map and its grid spacing were calculated from the nominal magnification of the electron microscope and the resolution of the micrograph scanner. Any inaccuracy in these numbers will lead to an uncertainty in the map magnification, and will consequently distort the correlation measurement between the model and the density map. In a preliminary investigation of the adverse effect introduced by this uncertainty, the magnification of the synthetic maps at 20 Å resolution used in the accuracy test (see Section 2) were artificially increased or decreased by 5% (data not shown).

The same procedure was then applied to refine the displaced model against the re-sized maps. The results were compared with those obtained from the maps of correct magnification. This simulation indicates that the error introduced to a refinement by an incorrect magnification value is less than 0.25 Å when the map is magnified by 5%, but increases to around 1.0 Å when the map is demagnified by 5%. Because this error varies with map resolution and sampling rate, a more rigorous investigation is currently underway.

The performance of the RSMD method depends on the quality of the density maps (Chen et al., 1999b). When a multi-subunit complex is modeled, the refinement of an atomic model can be further complicated if only parts of the complex are known in atomic detail. To improve the performance of the RSMD method, particularly under low SNR conditions, a multi-resolution refinement scheme has been proposed to increase the convergence radius.

Due to the uncertainty in the SNR and resolution measurement for experimentally obtained EM density data (Grigorieff, 2000), quantitative evaluation of a refined model is difficult. Although a global correlation coefficient is a quality indicator, it alone does not provide adequate information for a comprehensive assessment and, most importantly, does not prevent potential data over-fitting. Following the concept of cross-validation, a free R-factor, similar to that frequently quoted in X-ray crystallography structure refinement (Brünger, 1992b), has recently been developed for structural analysis in EM (Shaikh et al., 2003b). Other means, like difference maps and regional correlation indices, might also be employed to assess the progress of a refinement.

Acknowledgments

References

Bottcher, B., Wayne, S.A., Crowther, R.A., 1997. Determination of the fold of the core protein of hepatitis B virus by electron cryomicroscopy. Nature 385, 26–27.

Brünger, A.T., 1992a. X-PLOR Version 3.1: A System for X-ray Crystallography and NMR. Yale University Press, New Haven.

Brünger, A.T., 1992b. Free R value: a novel statistical quantity for assessing the accuracy of crystal structures. Nature 355, 472–475.

Brünger, A.T., Kuriyan, J., Karplus, M., 1987. Crystallographic R factor refinement by molecular dynamics. Science 235, 458–460.

Brünger, A.T., Adams, P.D., Clore, G.M., DeLano, W.L., Gros, P., Grosse-Kunstleve, R.W., Jiang, J.S., Kuszewski, J., Nilges, M., Pannu, N.S., Reed, R.J., Rice, L.M., Simonson, T., Warren, G.L., 1998. Cyrstallography & NMR system: a new software suite for macromolecular strcuture determination. Acta Crystallogr. D 54, 905–921.

Chapman, M.S., 1995. Restrained real-space macromolecular atomic refinement using a new resolution-dependent electron-density function. Acta Crystallogr. A 51, 69–80.

Chen, J.Z., Chapman, M.S., 2001. Conformational disorder of proteins assessed by real space molecular dynamics refinement. Biophys. J. 80, 1466–1472.

Chen, J.Z., Blanc, E., Chapman, M.S., 1999a. Real space molecular dynamics structural refinement. Acta Crystallogr. D 55, 464–468.

Chen, J.Z., Blanc, E., Chapman, M.S., 1999b. Improved free R-factors for the cross validation of macromolecular structures. Acta Crystallogr. D 55, 219–224.

Chen, L.F., Blanc, E., Chapman, M.S., Taylor, K.A., 2001. Real space refinement of acto-myosin structures from sectioned muscle. J. Struct. Biol. 133, 221–232.

Chiu, W., Rixon, F.J., 2002. High resolution structural studies of complex icosahedral viruses: a brief overview. Virus Res. 82, 9–17.

Egelman, E., DeRosier, D., 2003. Personal communication.

Frank, J., Agrawal, R.K., 2000. A ratchet-like inter-subunit reorganization of the ribosome during translocation. Nature 406, 318–322.

Frank, B.S., Vardar, D., Chishti, A.H., McKnight, C.J., 2003. The NMR structure dematin headpiece reveals a dynamic loop that is conformationally altered upon phosphorylation at a distal site, personal communication.

Frank, J., Radermacher, M., Penczek, P., Zhu, J., Li, Y., Ladjadj, M., Leith, A., 1996. SPIDER and WEB: processing and visualization of images in 3D electron microscopy and related fields. J. Struct. Biol. 116, 190–199.

Fürst, J., Sutton, R.B., Chen, J.Z., Brünger, A.T., Grigorieff, N., 2003. Electron cryo-microscopy structure of *N*-ethyl maleimide sensitive factor at 11 Å resolution. EMBO J. 22, 4365–4374.

Gao, H., Sengupta, J., Valle, M., Korostelev, A., Eswar, N., Stagg, S.M., Roey, P.V., Agrawal, R.K., Harvey, S.C., Sali, A., Chapman, M.S., Frank, J., 2003. Study of the structural dynamics of the *E. Coli* 70S ribosome using real-space refinement. Cell 113, 789–801.

Golas, M.M., Sander, B., Will, C.L., Luhrmann, R., Stark, H., 2003. Molecular architecture of the multiprotein splicing factor SF31. Science 300, 980–984.

Grigorieff, N., 2000. Resolution measurement in structures derived from single particles. Acta Crystallogr. D 56, 1270–1277.

Grigorieff, N., Ceska, T.A., Downing, K.H., Baldwin, J.M., Henderson, R., 1996. Electron-crystallographic refinement of the structure of bacteriorhodopsin. JMB 259, 393–421.

Hanson, P.I., Roth, R., Morisaki, H., Jahn, R., Heuser, J.E., 1997. Structure and conformational changes in NSF and its membrane receptor complexes visualized by quick-freeze/deep-etch electron microscopy. Cell 90, 523–535.

Harauz, G., van Heel, M., 1986. Exact filters for general geometry three-dimensional reconstruction. Optik 73, 146–156.

Henderson, R., Baldwin, J.M., Ceska, T.A., Zemlin, F., Beckmann, E., Downing, K.H., 1990. An atomic model for the structure of bacteriorhodopsin. Biochem. Soc. Trans. 18, 844.

Huang, C.C., Couch, G.S., Pettersen, E.F., Ferrin, T.E., 1996. Chimera: an extensible molecular modeling application constructed using standard components. Pac. Symp. Biocomput. 1, 724.

Janin, J., Henrick, K., Moult, J., Eyck, L.T., Sternberg, M.J.E., Vajda, S., Vakser, I., Wodak, S.J., 2003. CAPRI: a critical assessment of predicted interactions. Proteins: Struct. Funct. Genet. 52, 2–9.

Jiang, W., Baker, M.L., Ludtke, S.J., Chiu, W., 2001. Bridging the information gap: computational tools for intermediate resolution structure interpretation. J. Mol. Biol. 308, 1033–1044.

Kabsch, W., Mannherz, H.G., Suck, D., Pai, E.F., Holmes, K.C., 1990. Atomic structure of the Actin:DNAse I complex. Nature 347, 37–44.

Korostelev, A., Bertram, R., Chapman, M.S., 2002. Simulated annealing real-space refinement as a tool in model building. Acta Crystallogr. D 58, 761–767.

Lenzen, C.U., Steinmann, D., Whiteheart, S.W., Weis, W.I., 1998. Crystal structure of the hexamerization domain of *N*-ethylmaleimide-sensitive fusion protein. Cell 94, 525–536.

Miyazawa, A., Fujiyoshi, Y., Stowell, M., Unwin, N., 1999. Nicotinic acetylcholine receptor at 4.6 Å resolution: transverse tunnels in the channel wall. J. Mol. Biol. 288, 765–786.

Morgan, D.G., Macnab, R.M., Francis, N.R., DeRosier, D.J., 1993. Domain organization of the subunit of the *Salmonella typhimurium* flagellar hook. J. Mol. Biol. 229, 79–84.

Rosenfeld, A., 1984. Multiresolution Image Processing and Analysis. Springer, Berlin.

Roseman, A.M., 2000. Docking structures of domains into maps from cryo-electron microscopy using local correlation. Acta Crystallogr. D 56, 1332–1340.

Rossmann, M.G., Bernal, R., Pletnev, S.V., 2001. Combining electron microscopic with X-ray crystallographic structures. J. Struct. Biol. 136, 190–200.

Samatey, F.A., Matsunami, H., Imada, K., Nagashima, S., Namba, K., 2003. Personal communication.

Saxton, W.O., Baumeisterm, W., 1982. The correlation averaging of a regularly arranged bacterial cell envelop protein. J. Microsc. 127, 127–138.

Shaikh, T.R., Thomas, D., Francis, N.R., DeRosier, D.J., 2003a. Personal communication.

Shaikh, T.R., Hegerl, R., Frank, J., 2003b. An approach to examining model dependence in em reconstructions using cross-validation. J. Struct. Biol. 142, 30–310.

Volkmann, N., Hanein, D., 1999. Quantitative fitting of atomic models into observed densities by electron microscopy. J. Struct. Biol. 125, 176–184.

Wriggers, W., Milligan, R.A., McCammon, J.A., 1999. Situs: a package for docking crystal structures into low-resolution maps from electron microscopy. J. Struct. Biol. 125, 185–195.

Yu, R.C., Hanson, P.I., Jahn, R., Brünger, A.T., 1998. Structure of the ATP-dependent oligomerization domain of *N*-ethylmaleimide sensitive factor complexed with ATP. Nat. Struct. Biol. 5, 803–811.